Power system frequency estimation techniques a comparative study

Hesham El-Refaie
Electrical Eng. Dept., Faculty of Eng., Alexandria University, Alexandria, Egypt

Six techniques for estimating power system frequency are presented in the paper. These techniques are Discrete Fourier Transform [1], Smart Discrete Fourier Transform [2], Modified Discrete Fourier Transform [3], Orthogonal Component method [4], Frequency Demodulation method [5], and Prony's method [6]. These techniques are tested with waveforms free of harmonics at fundamental frequencies close to power system frequency (49.5 Hz and 50.5 Hz) and at fundamental frequency far from power system frequency (45 Hz and 55 Hz). These techniques are also tested with waveforms corrupted with the third and fifth harmonics at the same fundamental frequencies used in testing the techniques with waveforms free of harmonics (49.5, 50.5, 45, and 55 Hz). The Matlab software package [7] is used in this study to generate the waveforms and to simulate the frequency estimation techniques. The main goal of this study is to select the technique having the performance necessary to cope with the requirements of future protection and control systems and robust enough to cope with the more demanding nature of modern power system conditions.

نعرض فى هذة المقالة دراسة مقارنة لاستخدام ستة تقنيات لتقدير قيمة تردد نظم القوى الكهربية ولقد تم اختبار هذة التقنيات عند ترددات قريبة من تردد نظم القوى الكهربية (٤٩و٥ و ٥١و٥ هرتز) وترددات بعيدة عن تردد تظم القوى(٤٥ و ٥٥ هرتز) باستخدام موجات جيبية خالية من التوافقيات وموجات جيبية لها توافقيات ثلاثية و توافقيات خماسية ولقد تم استخدام برنامج ماتلاب لتوليد الموجات الجيبية وتمثيل التقنيات مع حساب الزمن اللازم لإجراء العمليات الحسابية لكل تقنية بواسطة وحدة المعالجة المركزية و الغرض من هذة الدراسة هو اختيار التقنية التى تتناسب مع متطلبات نظم الوقاية والتحكم الحديثة

Keywords: Frequency measurements, Power system harmonics, Discrete fourier transform, Orthogonal components, Frequency demodulation, Prony's method

1. Introduction

Discrete Fourier Transform (DFT) is not accurate when it is used in the case of asynchronous sampling. ref. [1] uses phase angle error caused by asynchronous sampling frequency for frequency tracking and phasor estimation. But in this paper the phase angle error taking account is incomplete. Thus, the frequency calculation and phasor estimation results are not precise.

The Smart Discrete Fourier Transform (SDFT) method developed in [2] takes into account of DFT errors completely, but it is complicated to calculate, especially in the presence of noise and higher order harmonics. Its complexity indicates its impracticality. Comprehensive analysis of DFT is given in [3]:
1. Why it is accurate when used in the case of synchronous sampling (synchronous sampling means that the sampling frequency is synchronized to analog signal frequency) and
2. How error rises in the case of asynchronous sampling. Simple but precise expressions of phase angle error and amplitude error are given. Practical formulas to calculate the true phase angle and amplitude are presented. The formulas are very simple and precise. Based on the formula to calculate true phase angle, a frequency tracking and phasor method was developed. This method can be calculated recursively, and with notable accuracy improvement. The calculation burden of this method is little more than the traditional DFT method.

The algorithm based on signal orthogonal components measurements is presented in [4]. This algorithm is based on the study of Moore, et al. given in ref. [8]. This study requires relatively high sampling rate of the input signal. Besides, proper numerical correction of both discrete derivative representation and orthogonal filters gains is necessary to obtain satisfactory accuracy of frequency estimation.

The algorithm given in [4] has been derived using finite differences rather than derivatives so it requires neither high signal sampling rate nor derivatives correction. Moreover, the varying filters frequency response does not affect the accuracy of frequency deviation measurement and thus no filter gains correction is necessary.

A method for frequency estimation in power system by demodulation of two complex signals is presented in [5]. The α-β transformation is used to convert three phase quantities to a complex quantity where the real part is the in-phase component and the imaginary part is the quadrature component. This complex is demodulated with a known complex phasor rotating in opposite direction to the input. The advantage of this method is that the demodulation does not introduce a double frequency component. For signals with high signal to noise ratio, the filtering demand for double frequency component can often limit the speed of the frequency estimation. Hence, the method can improve fast frequency estimation of signals with good noise properties.

A technique for estimating power system frequency based on Prony's method is presented in [6]. Prony's method is considered a powerful tool to analyze a signal and extract its modal information. This method can be used to analyze time independent signals and damped signals. The fact that Prony can handle damped signals and estimate the damping coefficients makes it suitable for applications based on power system transients. Prony calculates the modal information such as frequency, amplitude, damping and phase shift. These can be used to reconstruct the original signal or to make inferences about system conditions.

The organization of this paper is as follows:- The six techniques for estimating power system frequency are described briefly in section II. Simulation results to demonstrate the feasibility, precision, robustness, and simplicity of the techniques are presented in section III. The conclusions are presented in section IV.

2. Power system frequency estimation techniques

The six techniques for estimating power system frequency are presented in this section. A brief description of each technique is given.

2.1. Discrete Fourier transform

Consider a sinusoidal input signal of frequency ω given by

$$x(t) = \sqrt{2}X \sin(\omega t + \phi) . \quad (1)$$

Assuming that $x(t)$ is sampled N times per cycle of 50 Hz waveform to produce the sample set $\{x_k\}$

$$x_k = \sqrt{2}X \sin(\frac{2\pi}{N} K + \phi) . \quad (2)$$

The Discrete Fourier Transform of $\{x_k\}$ contains a fundamental frequency component given by

$$\overline{X}_1 = \frac{2}{N} \sum_{K=0}^{N-1} x_k e^{-j\frac{2\pi}{N}k} \quad (3)$$

$$= \frac{2}{N}\sum_{k=0}^{N-1} x_k \cos\frac{2\pi}{N}k - j\frac{2}{N}\sum_{k=0}^{N-1} x_k \sin\frac{2\pi}{N}k = X_c - jX_s , \quad (4)$$

where X_c and X_s are the cosine and sine multiplied sums in the expression for $\overline{X}_1$. It was shown in ref. [1] that the phasor representation of a sinusoidal signal is related to the fundamental frequency component of its DFT by

$$\overline{X} = \frac{1}{\sqrt{2}} j\overline{X}_1 = \frac{1}{\sqrt{2}}(X_s + jX_c) . \quad (5)$$

It was also shown in ref. [1] that it is possible to calculate the phasor recursively from the following equation:-

$$\overline{X}^r = \overline{X}^{(r-1)} + j\frac{1}{\sqrt{2}}\frac{2}{N}(x_{N+r} - x_r)e^{-j\frac{2\pi}{N}(r-1)} . \quad (6)$$

If the input signal frequency is now assumed to change slightly from 50 Hz by an amount *Δf*, it was shown in ref. [1] that the recursive relation of eq. (6) changes into

$$\overline{X}^{(r)}_{50+\Delta f} = \overline{X}^{(0)}_{50} \frac{\sin\frac{\Delta f}{50}\pi}{N\sin\frac{\Delta f}{50}\frac{\pi}{N}} e^{j\frac{\Delta f}{50}\frac{2\pi}{N}r} , \quad (7)$$

where $\overline{X}^{(0)}_{50}$ is the initial computation of the phasor from 50 Hz input signal having the same magnitude as (50+*Δf*) Hz signal, *r* is the recursion number, and *N* is the number of samples in a period of 50 Hz wave. Eq. 7 shows that when the input signal frequency changes from 50 Hz to (50+*Δf*) *Hz*, the phasor obtained recursively undergoes two modifications:- a magnitude factor of $\left(\frac{\sin\frac{\Delta f\pi}{50}}{N\sin\frac{\Delta f}{50}\frac{\pi}{N}}\right)$); and phase factor of $\exp(j\frac{\Delta f}{50}\frac{2\pi}{N}r)$. The magnitude factor is independent of *r*, and is relatively small for small changes in frequency. However, the phase angle is far more sensitive to the frequency *Δf*, and provides a most direct measure of Δf. Denoting the phase factor by $\exp(j\varphi_r)$, where

$$\varphi_r = \frac{\Delta f}{50}\frac{2\pi}{N}r . \quad (8)$$

Thus the phase angle at r^th recursive computation directly depends on the frequency deviation and the recursion order *r*. Since *r* increases by 1 in each iteration, the recursive relation for φ_r becomes

$$\varphi_r = \varphi_{r-1} + \frac{\Delta f}{50}\frac{2\pi}{N} . \quad (9)$$

Further, the time interval between two iterations is $1/50N$ seconds to be detected and therefore the angular velocity of φ is given by

$$\frac{d\varphi}{dt} = \frac{\varphi_r - \varphi_{r-1}}{1/50N} = 2\pi\Delta f$$

radians/ second (10)

Then, the exact solution of the frequency becomes

$$f = 50 + \Delta f = 50 + \frac{1}{2\pi}\frac{d\varphi}{dt} . \quad (11)$$

2.2. Smart discrete Fourier transform

It was shown in ref. [2] that when the signal frequency changes slightly from 50 Hz by an amount *Δf*, the recursive relation of eq. (6) changes into

$$\overline{X}^{(r)} = \frac{\overline{X}}{N}\frac{\sin\frac{N\theta_1}{2}}{\sin\frac{\theta_1}{2}} e^{j\frac{\pi}{50N}(\Delta f(2r+N-1)+100r)} + \frac{\overline{X}^*}{N}\frac{\sin\frac{N\theta_2}{2}}{\sin\frac{\theta_2}{2}} e^{-j\frac{\pi}{50N}(\Delta f(2r+N-1)+100(r+N-1))} . \quad (12)$$

where

$$\theta_1 = \frac{2\pi\Delta f}{50N} , \text{ and } \theta_2 = \frac{2\pi(2+\frac{\Delta f}{50})}{N}$$

If we define A_r and B_r as

$$A_r = \frac{\overline{X}}{N}\frac{\sin\frac{N\theta_1}{2}}{\sin\frac{\theta_1}{2}} e^{j\frac{\pi}{50N}(\Delta f(2r+N-1)+100r)} . \quad (13)$$

$$B_r = \frac{\overline{X}^*}{N}\frac{\sin\frac{N\theta_2}{2}}{\sin\frac{\theta_2}{2}} e^{-j\frac{\pi}{50N}(\Delta f(2r+N-1)+100(r+N-1))} . \quad (14)$$

Then eq. (12) can be expressed as

$$\overline{X}^{(r)} = A_r + B_r \,. \tag{15}$$

In the conventional DFT, it is assumed that the frequency deviation is small enough to be ignored, and $\overline{X}^{(r)} = A_r$. However, in the SDFT we take B_r into consideration. So we define

$$a = e^{j(\frac{\pi}{50N}(2\Delta f + 100))} \,. \tag{16}$$

and from eq. (13 and 14), we can find the following relations

$$A_{r+1} = A_r * a \,. \tag{17}$$

$$B_{r+1} = B_r * a^{-1} \,. \tag{18}$$

Then

$$\overline{X}^{(r+1)} = A_{r+1} + B_{r+1} = A_r * a + B_r * a^{-1} \,. \tag{19}$$

$$\begin{aligned}\overline{X}^{(r+2)} &= A_{r+2} + B_{r+2} = A_{r+1} * a + B_{r+1} * a^{-1} \\ &= A_r * a^2 + B_r * a^{-2} .\end{aligned} \tag{20}$$

There are three unknowns in eq. (15, 19 and 20), and after some algebric manipulations we obtain:

$$\overline{X}^{(r+1)} * a^2 - (\overline{X}^{(r)} + \overline{X}^{(r+2)}) * a + \overline{X}^{(r+1)} = 0 \,. \tag{21}$$

Solve eq. (21) to obtain

$$a = \frac{(\overline{X}^{(r)} + \overline{X}^{(r+2)}) \pm \sqrt{(\overline{X}^{(r)} + \overline{X}^{(r+2)})^2 - 4 * (\overline{X}^{(r+1)})^2}}{2 * \overline{X}^{(r+1)}} \,. \tag{22}$$

Then from the definition of “a” in eq. (16), we can obtain the exact solution of the frequency as

$$f = 50 + \Delta f = \cos^{-1}(\mathrm{Re}(a)) * \frac{50N}{2\pi} \,. \tag{23}$$

2.3. Modified discrete Fourier transform

It was shown in ref. [3] that when the signal frequency changes slightly from 50 Hz by an amount Δf, the relationship between the phase angle calculated by DFT and the actual one is given by

$$\varphi = \varphi_m - \Delta f \pi \frac{N-1}{N} - \frac{\Delta f \pi}{N \sin(\frac{2\pi}{N})} \sin(\frac{2\pi}{N} - 2\varphi_m) , \tag{24}$$

where φ is the actual phase angle and φ_m is the phase angle calculated by DFT.

Eq. (24) is the basic for frequency tracking algorithm presented in ref. [3]. In this algorithm, the signal *x(t)* is sampling with sampling period T_s to produce *x(n)*

$$x(n) = x(t)\big|_{t=nT_s} \qquad (-\infty<n<\infty) , \tag{25}$$

$x(n)$ is windowing with rectangular windows $d(n)$ and $d(n-M)$ to produce two sequences of length N

$$x_d(n) = x(n) * d(n) ,\; x_d^M(n) = x(n) * d(n-M) \,. \tag{26}$$

The phasor representation of $x_d(n)$ and $x_d^M(n)$ are

$$\overline{X}_1 = X * e^{j\varphi_1} ,\quad \overline{X}_2 = X * e^{j\varphi_2} , \tag{27}$$

where φ_1 and φ_2 are true phase angles of $\overline{X}_1$ and $\overline{X}_2$. They have the following relationship:

$$\varphi_1 - \varphi_2 = \frac{2\pi M T_s}{T} = \frac{(1+\Delta f) 2\pi M}{N} , \tag{28}$$

where T is the time period of the signal.
According to eq. (24), we have

$$\varphi_{1m} = \varphi_1 + \Delta f \pi \frac{N-1}{N} + \frac{\Delta f \pi}{N \sin(\frac{2\pi}{N})} \sin(\frac{2\pi}{N} - 2\varphi_{1m}) . \tag{29}$$

$$\varphi_{2m} = \varphi_2 + \Delta f \pi \frac{N-1}{N} + \frac{\Delta f \pi}{N \sin(\frac{2\pi}{N})} \sin(\frac{2\pi}{N} - 2\varphi_{2m}). \quad (30)$$

where φ_{1m} is the calculated phase angle of phasor $\overline{X}_1$ and φ_{2m} is the calculated phase angle of $\overline{X}_2$.

Define

$$K = \frac{\pi}{N \sin(\frac{2\pi}{N})}. \quad (31)$$

$$K_1 = \sin(\frac{2\pi}{N} - 2\varphi_{1m}). \quad (32)$$

$$K_2 = \sin(\frac{2\pi}{N} - 2\varphi_{2m}). \quad (33)$$

$$K_3 = \frac{2\pi M}{N}. \quad (34)$$

From eq. (29 and 30).

$$\varphi_{2m} - \varphi_{1m} = (1 + \Delta f) K_3 + K(K_2 - K_1)\Delta f. \quad (35)$$

The solution of eq. (35) is

$$\Delta f = \frac{(\varphi_{2m} - \varphi_{1m}) - k_3}{K_3 + K(K_2 - K_1)}. \quad (36)$$

The actual frequency of $x(t)$ is

$$f = \frac{f_s(1 + \Delta f)}{N}, \quad (37)$$

where f_s is the sampling frequency.

2.4. Orthogonal components

It was shown in ref. [4] that the orthogonal components can be obtained by processing the signal using a pair of orthogonal Finite Impulse Response (FIR) filters whose impulse responses should be even or odd, respectively. Such FIR filters reveal linear phase response and the difference of their digital transfer function arguments is equal to $\pi/2$ for all frequencies. It means that the filters are orthogonal for all frequencies. The filters process the input signal x and produce a pair of output orthogonals y_c, y_s according to the following equations:

$$y_c(n) = \sum_{i=0}^{N-1} x(n-i)\omega_c(i), \quad (38)$$

$$y_s(n) = \sum_{i=0}^{N-1} x(n-i)\omega_s(i), \quad (39)$$

where N is FIR order that is equal to the ratio of sampling and power system nominal frequencies (also a number of samples in one period of fundamental frequency component). ω_c and ω_s are even and odd impulse responses of FIR filters, respectively (sin and cos for example).

It was also shown in ref. [4] that the signal frequency can be calculated according to the formula:

$$f = 50\{1 - \frac{1}{\pi} \frac{y_s(n)y_c(n-2k) - y_c(n)y_s(n-2k)}{y_s(n)y_c(n-k) - y_c(n)y_s(n-k)}\}. \quad (40)$$

The delay k was chosen equal to $N/4$.

It is noting from eq. (40) that the estimated frequency does not depend on filter gains, sampling period T_s, and discrete derivative representation. Thus this technique does not require filter gain correction, derivative correction and high sampling rate (contrary to the algorithm [8] in which calculation and correction of signal first derivative calls for high sampling rates). The only requirement is that the number of samples N must be selected in such a way that $N/4$ is a natural number.

2.5. Frequency demodulation

Consider x_1, x_2, and x_3 to be samples of the three phase signal.-

$$x_i(k) = \sqrt{2} X \sin(\omega_1 t_k + \phi_i) + e_i(k)$$
i=1, 2, and 3. (41)

where e_i is a general noise term that can be any combination of white noise and harmonics.

The α, β components are defined as the complex phasor.

$$V(k) = V_\alpha(k) + jV_\beta(k), \quad (42)$$

where the real and imaginary parts are calculated from

$$\begin{bmatrix} V_\alpha \\ V_\beta \end{bmatrix} = \sqrt{\frac{2}{3}} \begin{pmatrix} 1 & -\frac{1}{2} & -\frac{1}{2} \\ 0 & \frac{\sqrt{3}}{2} & -\frac{\sqrt{3}}{2} \end{pmatrix} \begin{bmatrix} x_1(k) \\ x_2(k) \\ x_3(k) \end{bmatrix}. \quad (43)$$

In the literature, the complete transformation is often called α, β, 0 transform and also includes the zero sequence component. In our application we only use the two perpendicular parts α and β and therefore leave out the zero sequence component in our transformation.

To make the analysis straightforward we first assume that the input signals x_1, x_2, and x_3 do not have any negative sequence component nor any noise. We then have

$$V(k) = A[\cos(\omega_1 t_k + \phi) + j\sin(\omega_1 t_k + \phi)] = Ae^{j(\omega_1 t_k + \phi)}, \quad (44)$$

where A is the phase to phase RMS value.
The demodulation is done with a complex signal Z, that rotates in the opposite direction, i. e. , negative sequence, compared to the input signal V.
The signal Z with a known frequency ω_0 is

$$Z(k) = \cos(-\omega_0 t_k) + j\sin(-\omega_0 t_k) = e^{-j\omega_0 t_k}. \quad (45)$$

The resulting signal after multiplication becomes

$$Y(k) = V(k)\cdot Z(k) = Ae^{j(\omega_1 t_k + \phi)}e^{-j\omega_0 t_k} = Ae^{j[(\omega_1 - \omega_0) + \phi]}$$
$$= A\{\cos[(\omega_1 - \omega_0)t_k + \phi] + j\sin[(\omega_1 - \omega_0)t_k + \phi]\}. \quad (46)$$

Note that the demodulation does not create the double frequency component. Hence, the demodulation does not add demands to filter away the double frequency component. However, there still might be a need to filter due to noise. To find the phase difference, we define the complex variable U as

$$U(k) = Y(k)\cdot Y(K-1)^*, \quad (47)$$

where* stands for conjugate. We separate Y in real and imaginary and find that

$$U(k) = \mathrm{Re}[Y(k)]\,\mathrm{Re}[Y(k-1)] + \mathrm{Im}[Y(k)]\,\mathrm{Im}[Y(k-1)] + j\{\mathrm{Im}[Y(k)]\,\mathrm{Re}[Y(k-1)] - \mathrm{Re}[Y(k)]\,\mathrm{Im}[Y(k-1)]\}. \quad (48)$$

The phase difference γ between two consecutive samples is calculated from the real and imaginary parts of U.

$$\gamma(k) - \gamma(k-1) = \arctan\left(\frac{\mathrm{Im}[U(k)]}{\mathrm{Re}[U(k)]}\right). \quad (49)$$

The deviation in angular frequency is estimated from

$$\Delta\omega(k) = \frac{1}{T_s}[\gamma(k) - \gamma(k-1)] = f_s[\gamma(k) - \gamma(k-1)]. \quad (50)$$

The unknown frequency of the signal V is estimated as

$$f = f_0 + \frac{f_s}{2\pi}\arctan\left(\frac{\mathrm{Im}[U(k)]}{\mathrm{Re}[U(K)]}\right), \quad (51)$$

where f_0 is the nominal and, f_s is the sampling frequency.

2.6. Prony's method

It is shown in ref. [9] that the sinusoidal signal can be expressed by q_1 real terms, corresponding to purely damped exponential, and q_2 complex terms plus their conjugates:

$$x_n = \sum_{k=1}^{p} \beta_k z_k^n \quad n = 0, 1, \ldots, N-1, \quad (52)$$

where p is the signal order ($p = q_1 + 2q_2$), β_k is the complex magnitude, and z_k, is the complex frequency. β_k and z_k can be written in terms of real parameters as follows:

$\beta_k = A_k\, e^{j\theta_k}$ for purely damped exponentials

$\beta_k = 1/2\, A_k\, e^{j\theta_k}$ for pure and damped sinusoids

$$z_k = e^{(-\alpha_k + j2\Pi f_k)\Delta T} . \quad (53)$$

The 3-step Prony analysis identifies the 'p' distinct eigen values (λ_ks) and signal residues (β_ks) according to the following procedure:

Step I: Coefficients estimation

Linear Prediction Model (LPM) construction in which the signal can be described by:

$$x(n) = \sum_{k=1}^{L} a_k x(n-k) , \quad (54)$$

where: n=L+1…N.

L: is an integer such that $L >> p$.

Eq. (56) can be written in the following matrix form in which the coefficients $[a_k]_{k=1 \to L}$ are the unknowns.

$$[h_1].\ [a_k] = [H], \quad (55)$$

where

$$[h_1] = \begin{bmatrix} X(L) & X(L-1) & \cdots & X(1) \\ X(L-1) & & & \vdots \\ \vdots & & & \vdots \\ X(N-1) & & & X(N-L) \end{bmatrix},$$

$$[a_k] = \begin{bmatrix} a_1 \\ a_2 \\ \vdots \\ a_L \end{bmatrix}, \text{ and } [H] = \begin{bmatrix} X(L+1) \\ X(L+2) \\ \vdots \\ X(N) \end{bmatrix}.$$

The least square estimator for the coefficients 'a_ks' can be obtained using the pseudo inverse of hankel matrix $[h_1]$.

Step II: Polynomial root finding

Solving the characteristic polynomial associated with LPM. The eigen values can be obtained using the roots (Z_k^k) of the equation.

$$f(z) = \prod_{k=1}^{L} (z - z_k) = (z - z_1)(z - z_2)\ldots(z - z_L)$$

$$\text{or } z^L - (a_1 z^{L-1} + a_2 z^{L-2} + \ldots + a_L) = 0. \quad (56)$$

Step III: Signal residue estimation

Using the roots obtained as the complex modal frequencies for the signal, we can determine the signal residues for each mode according to the equation:

$$\vec{x} = \upsilon.\vec{B} , \quad (57)$$

υ: is a Vander mode matrix.

Where

$$\vec{x} = \begin{bmatrix} x(1) \\ x(2) \\ \vdots \\ x(N) \end{bmatrix}, \ \upsilon = \begin{bmatrix} z_1 & z_2 & \cdots & z_p \\ z_1^2 & z_2^2 & \cdots & z_p^2 \\ \vdots & & & \vdots \\ z_1^N & z_2^N & & z_p^N \end{bmatrix}, \text{ and}$$

$$\vec{B} = \begin{bmatrix} B_1 \\ B_2 \\ \vdots \\ B_P \end{bmatrix}$$

The least square method is applied to yield the solution

$$\vec{B} = (\upsilon^T \upsilon)^{-1} \upsilon^T .\vec{x} . \quad (58)$$

Prony's method is completed with computation of the frequency:

$$f_k = \frac{angle(z_k)}{2\Pi\Delta t} \qquad k = 1\ldots q. \quad (59)$$

3. Simulation results

The six techniques are tested with sinusoidal waveforms free of harmonics at frequencies close to power system frequency (49.5 Hz and 50.5 Hz), and at frequencies far of power system frequencies (45 Hz and 55Hz). These techniques are also tested with waveforms corrupted with third and fifth harmonics at the same frequencies (45.5, 50.5, 45, and 55 Hz) used in testing the techniques with waveforms free from harmonics. The Matlab [7] software package is used to generate waveforms and to simulate frequency estimation techniques. The computation time of each technique is calculated and used also in testing the six techniques.

3.1. Testing the techniques with sinusoidal wave forms free from harmonics

The six techniques are tested with sinusoidal waveforms free of harmonics and the simulation results are shown in fig. 1. The following remarks are observed from these results:-

1. The 50 Hz frequency is correctly estimated by DFT as shown in Fig. 1-a. But when this technique is used for estimating 49.5, 50.5, 45, 55 Hz frequencies, the deviations between the calculated values and true values are large.
2. The 45, 49.5, 50, 50.5, and 55 Hz frequencies are correctly estimated by smart discrete fourier transform as shown in fig. 1-b.
3. The 49.5, 50, and 50.5 Hz frequencies are correctly estimated by Modified Discrete Fourier Transforms as shown in fig. 1-c. But when this technique is used for estimating 45 and 55 Hz, oscillations are observed in the estimated values. The amplitudes of these oscillations are smaller than those shown in fig. 1-a.
4. The 45, 49.9, 50, 50.5, and 55 Hz frequencies are correctly estimated by the technique of orthogonal components as shown in fig. 1-d.
5. When the frequency demodulation technique is used for estimating 45, 49.5, 50, 50.5, and 55 frequencies, oscillations are observed in the estimated values as shown in fig. 1-e. The amplitudes of these oscillations are smaller than those shown in fig. 1-a.
6. The 45, 49.9, 50, 50.5, and 55 Hz frequencies are correctly estimated by the Prony's method as shown in fig. 1-f.

3.2. Testing the techniques with waveforms corrupted by harmonics

The six techniques are tested with sinusoidal waveforms corrupted by third and fifth harmonics and the simulation results are shown in fig. 2. The following remarks are observed from these results:-

1. The 50 Hz frequency is correctly estimated by the DFT as shown in fig. 2-a. But when this technique is used for estimating 45, 49.5, 50.5, and 55 Hz, the deviations between the calculated values and true values are large. These results are similar to those shown in fig. 1-a.
2. The 50 Hz frequency is correctly estimated by Smart Fourier Transform as shown in fig. 2-b. But when this technique is used for estimating 45, 49.5, 50.5, and 55 Hz, the deviations between the calculated values and actual values are large. The frequencies estimated by this technique are deviated from actual values when the sinusoidal waveforms used in the test corrupted by harmonics but they are closed to actual values when the sinusoidal waveforms are free from harmonics.
3. The results of estimating frequencies by Modified Discrete Fourier Transform shown in fig. 2-c are similar to those shown in fig. 1-c. The estimated frequencies by this technique are the same whether the sinusoidal waveforms used in the test free or corrupted by harmonics.
4. The 49.5, 50, and 50.5 Hz frequencies are correctly estimated by the technique of Orthogonal Components as shown in fig. 2-d. These results are similar to those shown in fig. 1-d. But when this technique is used for estimating 45 and 55 Hz, small oscillations are observed in the estimation values. The 49.5, 50, 50.5 Hz are correctly estimated by this technique whether the sinusoidal waveforms are free or corrupted by harmonics. But when it used for estimating 45 and 55 Hz small oscillations are observed in the estimation values if the waveforms used in the test are corrupted by harmonics.
5. When the frequency demodulation technique is used for estimating 45, 49.5,50,50.5, and 55 Hz in presence of harmonics, the deviation between actual and estimated values are large as shown in fig. 2-e.
6. When the Prony's method is used for estimating 45, 49.5, 50, 50.5, and 55 Hz in presence of harmonics, the estimated values are closed to actual values as shown in fig. 2-f.

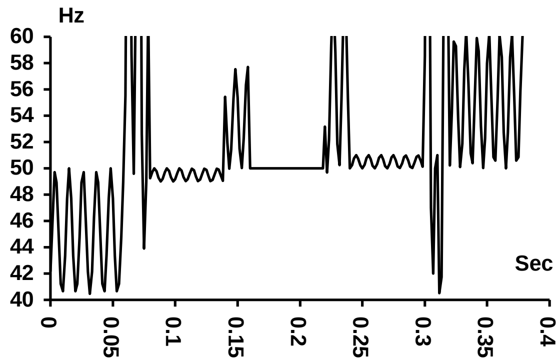

(a) Discrete fourier transform technique.

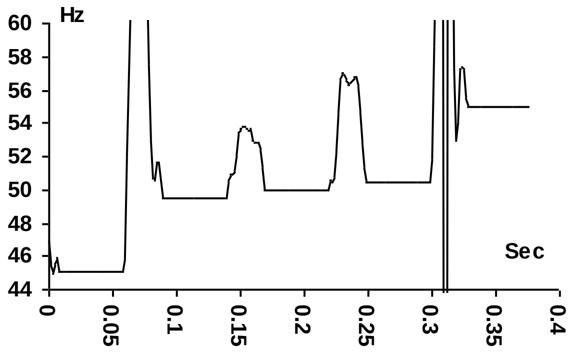

(d) Orthogonal components.

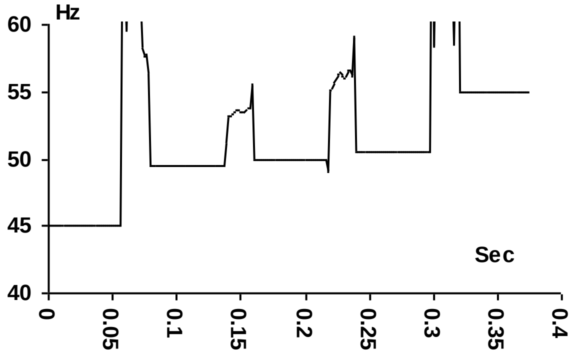

(b) Smart Discrete Fourier transform.

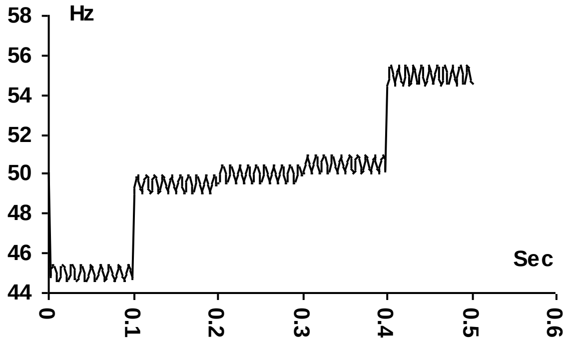

(e) Frequency Demodulation technique.

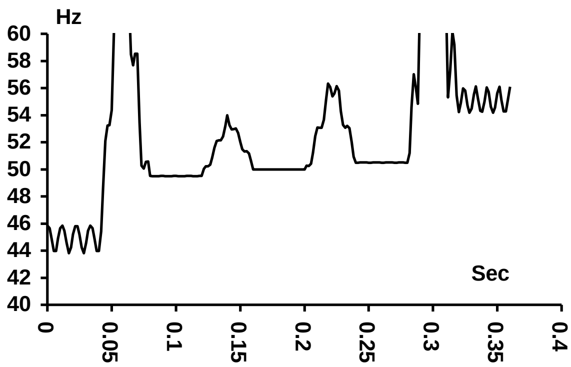

(c) Modified Fourier transform.

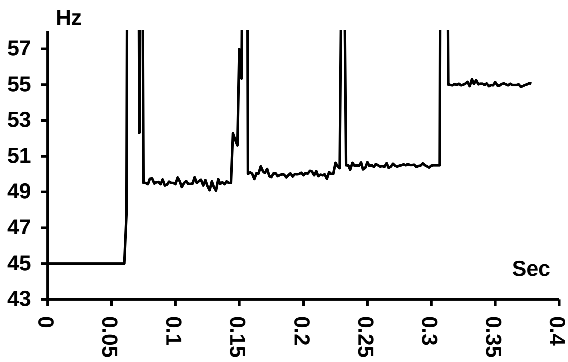

(f) Prony's method.

Fig.1. Test of the techniques with sinusoidal waveforms free from harmonics.

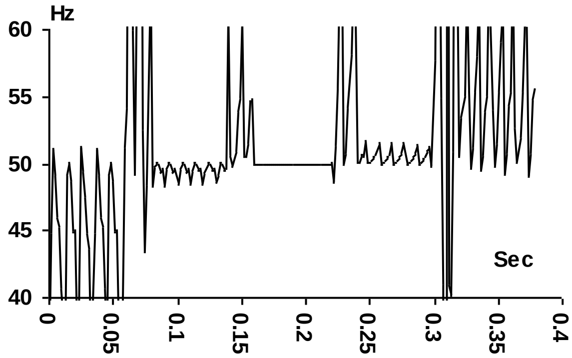

(a) Discrete Fourier transform technique.

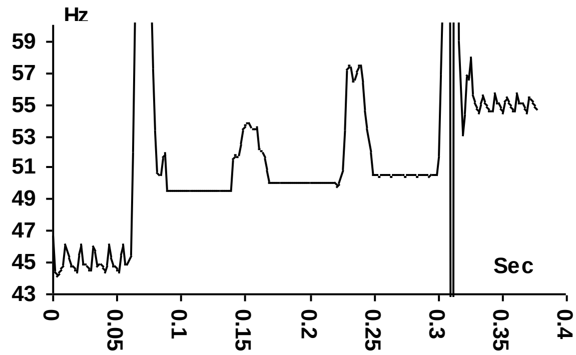

(d) Orthogonal components.

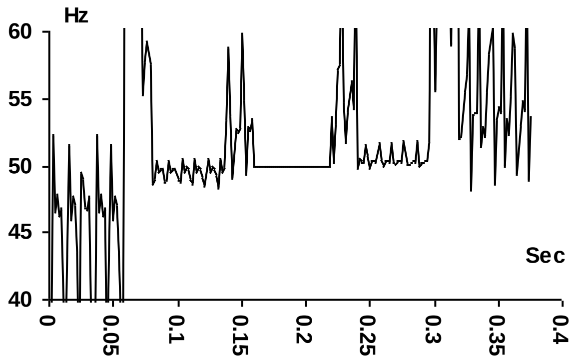

(b) Smart discrete Fourier transform.

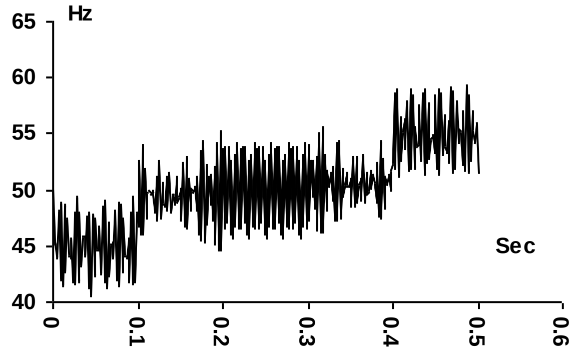

(e) Frequency demodulation technique.

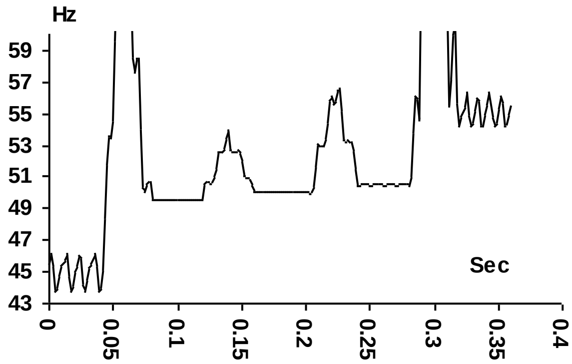

(c) Modified Fourier transform.

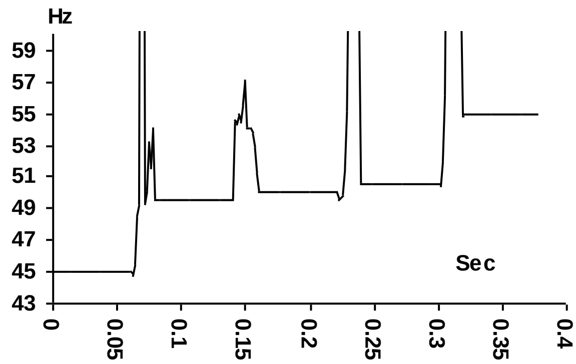

(f) Prony's method.

Fig. 2. Test of the techniques with sinusoidal waveforms corrupted by harmonics.

Table 1
Computation time

The method	Discrete Fourier transform	Smart discrete Fourier transform	Modified discrete Fourier transform	Orthogonal components	Frequency demodulation	Prony's method
Time (Sec)	1.7	2.58	1.76	0.11	0.05	6.71

3.3. Computation time

Table 1 shows the CPU time of each technique. There are 240 data per 0.4 Sec. computed by each technique. We find that the frequency demodulation technique is the fastest one, but the estimated frequencies using this technique are largely deviated from the actual values. The slowest is Prony's method, but the estimated frequencies obtained by this technique are close to the actual values. The technique of Orthogonal Components is slower than Frequency Demodulation but is faster than other techniques. The estimated frequencies using this technique are close to actual values if it is used to estimate frequencies close to power system frequencies (49.5, 50, and 50.5 Hz) whether the waveforms used in the test are free or corrupted by harmonics. But when this technique is used for estimating frequencies far from power system frequencies (45 and 55 Hz), small oscillations are observed in the estimated values if the waveforms used in the test are corrupted by harmonics. Thus the technique of the Orthogonal Components is the most suitable one to cope with the requirements of future protection and control equipments.

4. Conclusions

A comparative study has been carried out to six techniques for estimating power system frequency. These techniques are tested at frequencies close to power system frequency and far from power system frequency with sinusoidal waveforms free and corrupted by harmonics. It is found that the computation time of Prony's method is the largest one but the estimated frequencies using this technique are close to actual values. The Frequency Demodulation technique has the smallest computation time but the estimated frequencies using this technique are far from the actual values. The computation time of the technique of Orthogonal Components is bigger than the frequency demodulation technique but it is smaller than other techniques. When this technique is used for estimating frequencies close to power system frequency, the estimation values are close to actual values whether the waveforms used in the test are free or corrupted by harmonics. But when this technique is used for estimating frequencies far from power system frequency, small oscillations are observed in the estimation values if the waveforms used in the test are corrupted by harmonics. Thus the technique of Orthogonal Components is the most suitable one to cope with future requirements of protection and control equipments.

References

[1] A.G. Phadke, J.S. Thorp and M.G. Adamiak, "A New Measurement Technique for Tracking Voltage Phasor, Local System Frequency, and Rate of change of Frequency", IEEE Transactions on Power Apparatus and Systems, Vol. PAS-102 (5), pp. 1025-1038 (1983).

[2] J.Z. Yang and W.L. Chih, "A Precise Calculation of Power System Frequency and Phasor", IEEE Transactions on Power Delivery, Vol. 15 (2), pp. 494-499 (2000).

[3] M. Wang, S. Yuanzhang, "A Practical, Precise Method for Frequency Tracking and Phasor Estimation", IEEE Transaction on Power Delivery, Vol. 19 (4), pp. 1547-1552 (2004).

[4] J. Szafran and W. Rebizant, "Power System Frequency Estimation", IEE Proceeding, Generation, Trasmission and Distribution, Vol. 141 (5), pp. 578-582 (1998).

[5] M. Akke, "Frequency Estimation by Demodulation of Two Complex Signals",

IEEE Transactions on Power Delivery, Vol. 12 (1), pp. 157-163 (1997).
[6] T. Lobos and J. Rezmer, "Real-Time Determination of Power System Frequency", IEEE Transactions on Instrumentation and Measurement, Vol. 46 (4), pp. 877-881 (1997).
[7] A. Cavallo, R. Setola and F. Vasco, Using Matlab, Simulink and Control System Toolbox, Prentice Hall (1994).
[8] P.J. Moore, R.D. Curranze and A.T. Johns, "A New Numeric Technique for High Speed Evaluation of Power System Frequency", IEE Proceeding, Generation, Transmission, and Distribution, Vol. 141 (5), pp. 529-536 (1994).
[9] O. Chaari, P. Bastard and M. Beunier, "Prony's Method: an Efficient Tool for the Analysis of Earth Currents in Peterson-Coil Protected Networks", IEEE Transactions on Power Delivery, Vol. 10 (5), pp. 1234-1241 (1995).

Received March 10, 2007
Accepted May 23, 2007